Advanced Composite Materials
Publication details, including instructions for authors and subscription information:
http://www.tandfonline.com/loi/tacm20

The influence of thermal shock on inter-laminar shearing strength of woven C/C composites

Hiroshi Fukuda , Go Itohiya , Jun Watanabe , Jun Takahashi & Kiyoshi Kemmochi

Version of record first published: 02 Apr 2012.

To cite this article: Hiroshi Fukuda , Go Itohiya , Jun Watanabe , Jun Takahashi & Kiyoshi Kemmochi (2000): The influence of thermal shock on inter-laminar shearing strength of woven C/C composites, Advanced Composite Materials, 9:2, 145-159

To link to this article: http://dx.doi.org/10.1163/15685510051029291

Adv. Composite Mater., Vol. 9, No. 2, pp. 145–159 (2000)

JSCM Award Winning Paper

The influence of thermal shock on inter-laminar shearing strength of woven C/C composites

HIROSHI FUKUDA [1], GO ITOHIYA [1], JUN WATANABE [2], JUN TAKAHASHI [3] and KIYOSHI KEMMOCHI [3]

[1] *Science University of Tokyo, Yamazaki, Noda 278-8510, Japan*
[2] *Nissan Motor Co., Ltd., Atsugi 243-0126, Japan*
[3] *National Institute of Materials and Chemical Research, 1-1, Higashi, Tsukuba 305-8586, Japan*

Received 3 February 1998; accepted 21 September 1999

Abstract—Although the mechanical properties of carbon fiber reinforced carbon (C/C) composites under high temperature environments have been widely studied to date, the influence of thermal shocks on C/C composites have scarcely been investigated due to the lack of high-speed heating equipment. Our equipment based on a high frequency induction heating method provided a solution to this problem. In the present study, we examined the influence of thermal shocks on the inter-laminar shearing strength (ILSS), which is one of the most important subjects of designing a plain woven C/C composite with a three point bending test. By the change of the span-to-height ratio (l/h), the failure mode shift of the inter-laminar shearing to the bending was observed. By a series of tests, we proposed an appropriate l/h ratio to obtain a reliable inter-laminar shearing strength of C/C composites, which would be higher than that for the conventional CFRPs. The observation of the failure specimens was done by scanning electron microscopy (SEM) and optical microscopy. Not only debondings at $0°/90°$ interface but also propagation of transverse cracks were observed in the thermal shocked specimens. The $0°/90°$ interfacial debondings were suggested as the main source of the inter-laminar shearing strength deterioration.

Keywords: C/C composites; woven fabric; thermal shock; three-point bending; interlaminar shearing strength; fractography; damage mechanism.

1. INTRODUCTION

As C/C composites (Carbon fiber-reinforced Carbon composites) are light weight and have superior properties in heat resistance, many studies have been conducted for the mechanical properties under high temperature environments. However, most available studies are under static heating (such as using an electric resistance heating system) and there are very few studies available on the influence of rapid thermal hysteresis (thermal shocks such as space plane reentry to atmosphere) and its repetition [1, 2] because of the restrictions of rapid heating that need to be

imposed on the heating device which makes a realistic simulation of thermal shocks very difficult. In this experiment, rapid heating of 200°C/s (about 300°C/s as the maximum) was realized by adopting a high-frequency induction heating method and with natural cooling (−150°C/s on the average, −200°C/s at the maximum) from high temperatures, simulations of more realistic thermal shocks were made possible.

In the previous report [1], a systematic study was conducted to investigate the effects of thermal design of this experimental apparatus (temperature distribution of the test specimens in the one-sided axial and cross-sectional directions) and the thermal shock on the temperature dependence of the infrared radiation rate, the thermal expansion coefficient, the tensile strength and the notch strength. It was revealed that the thermal shock significantly affected (1) the generation of microcracks (at rapid cooling) induced by the difference in thermal expansion coefficients between the fibers and the matrix and (2) delamination (at rapid heating) induced by the temperature gradient in the thickness direction of the test specimen upon thermal shocks.

In this paper, the effect of thermal shocks on the inter-laminar shearing strength (ILSS) of C/C composites was investigated based on the result of internal observation by SEM, because ILSS is an important factor in designing composites. The three-point testing method (the short beam method) and the double notch inter-laminar shearing test method are popular methods for testing [3] and the three-point bending test was adopted here in order to locate the boundary between the inter-laminar shearing failure and the bending failure of C/C composites.

2. EXPERIMENTAL

2.1. Test specimens and shapes

Table 1 shows the specification of the C/C composites used in this experiment. The test specimens were plain woven C/C composites fabricated by Owada Carbon Co. and the final heat treatment temperature (HTT) was 1600°C. The matrix phase was

Table 1.
Constituents of C/C composites

Composites	
Fiber	Matrix
Type: HTA No. of filaments: 3000	Base: Phenolic resin Densification: Coal-tar pitch
Plain woven fabric, No. of plies: 12 Vf: 60–65 vol% Heat treatment temperature: 1600°C Density: 1.5 g/cm^3	

densificated by coal-tar pitch with phenol resin as the base and the fibers were made of HTA (PAN family general purpose grade carbon fibers) fabricated by Toray.

The shape of the test specimens was short rectangular with the thickness of $h = 3$ mm, the width of $b = 8$ mm and the overhang length of $l' = 2$ mm. As there is no inter-laminar shearing stress, τ, on the overhang part of the test specimens, no delamination should take place theoretically. However, inter-laminar cracks do reach the overhang part in reality. It was found, however, that inter-laminar cracks did not propagate to the overhang part (delamination was present only between the loading nose and the support point) when a preliminary test was conducted based on the JIS standard (JIS K7078, the inter-laminar shearing test method of carbon fiber reinforced plastics) with the overhang length of the test specimen made the same as the specimen thickness ($h = 3$ mm). For this reason, the experiment was conducted with test specimens whose overhang length was 2 mm, shorter than the standard by 1 mm.

2.2. Experimental method

The (apparent) inter-laminar shearing strength before and after the thermal shocks was obtained by the three point bending test. The boundary between the inter-laminar shearing failure and the bending failure was also examined by varying the span/thickness ratios ($l/h = 4, 5, 6, \ldots, 20$). The relationship between the number of thermal shocks and the inter-laminar shearing strength was also investigated. The inter-laminar shearing strength, $\tau_{\max}$, and the bending strength, $\sigma_{\max}$, were calculated from the following formulas:

Inter-laminar shearing strength

$$\tau_{\max} = \frac{F}{I}\frac{h^2}{8} = \frac{3}{4}\frac{P}{bh}. \tag{1}$$

Bending strength

$$\sigma_{\max} = \frac{M}{I}\frac{h}{2} = \frac{3}{2}\frac{Pl}{bh^2}, \tag{2}$$

where F is the shearing force (N); I is the cross-sectional second order moment (m^4); M is the moment at bending failure (N m); P is the failure load (N); b is the width of test specimen (m); h is the thickness of the test specimen (m) and l is the span of the test specimen (m).

The failure load, P, was defined as the first peak load, not the maximum load because there was a possibility that continuation of load application beyond the first peak load may alter the failure morphology from the initial state [4]. Furthermore, if the size effect was neglected, the inter-laminar shearing stress, $\tau_{\max}$, and the bending strength, $\sigma_{\max}$, must be constant independent of the span, l. Even though the right hand side of equation (2) contains l, it simply implies that the failure load, P, is halved when l is doubled.

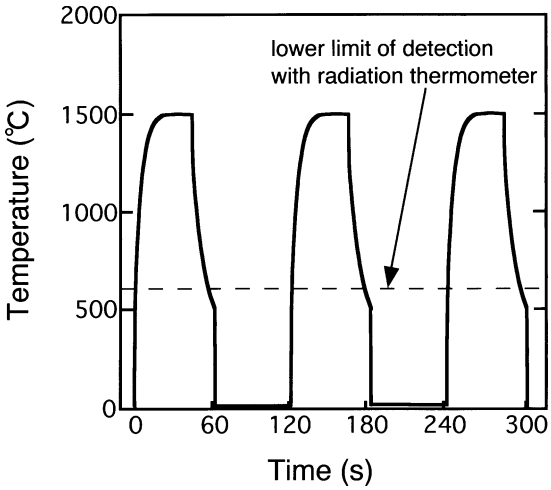

Figure 1. Temperature transition under thermal shock testing.

2.3. Experimental device

The loads were generated by a hydraulic tester (the EHF-FD5-10L type, manufactured by Shimadzu Co.) at the cross head speed of 0.5 mm/min. The radii of curvature of the ILSS test jigs (JIS K 7057) were chosen as 4 mm for the loading nose and 3 mm for the supporting point.

The high-frequency induction heating method was adopted [5] as the heating method. Heating was performed under nitrogen atmosphere inside the oven in order to prevent oxidation of C/C composites that may take place at temperatures above 500°C [6]. One thermal shock was defined as heating to 1500°C at an average of 200°C/s (maximum of about 300°C/s), keeping at 1500°C for about 20 s, and then cooling down to room temperature (at an average of −150°C/s for 20 s), and three thermal shocks were given to the test specimens. Figure 1 shows the temperature transition curve. A radiation temperature gauge (the IR-AP2Cs, manufactured by Chinon, Inc., measurement range: 600−3000°C) was used to measure the temperature.

3. RESULTS AND DISCUSSION

3.1. Inter-laminar shearing strength, τ_{max}, and bending strength, σ_{max}

Figure 2 shows a plot of the apparent inter-laminar shearing strength, $\tau_{\max}$, computed from equation (1) based on the failure load, P, when the ratios of span/thickness (l/h) were varied. The test data with bending failure are shown by the Δ symbols and those with inter-laminar failure are shown by the ○ and □ symbols while those after the thermal shocks are shown by the ▲, ● and ■ symbols. The failure mode was determined by eye inspection and sound when the specimens failed.

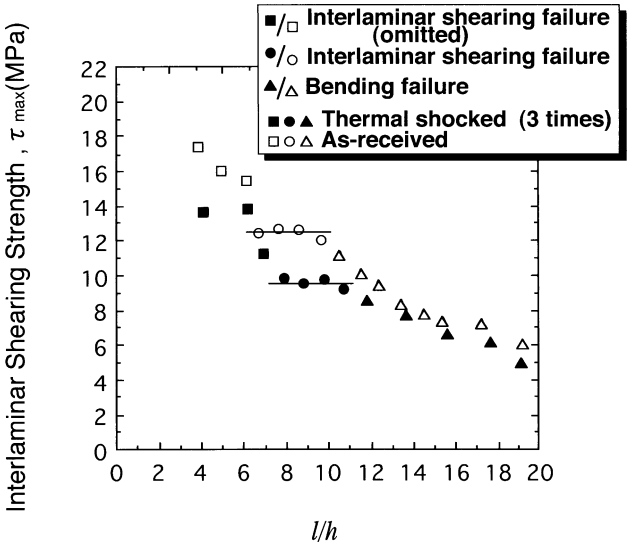

Figure 2. Comparison of inter-laminar shearing strength.

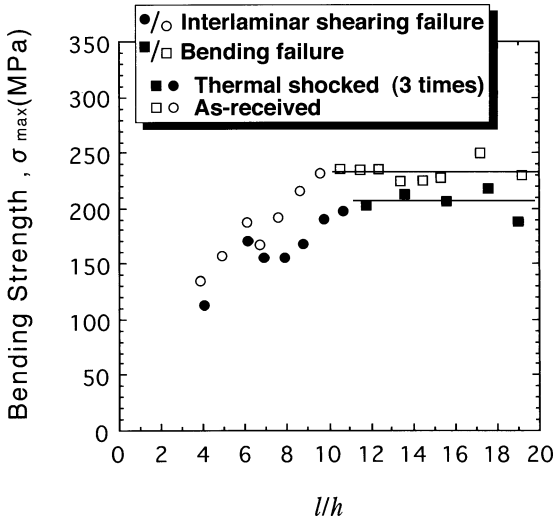

Figure 3. Comparison of bending strength.

The inter-laminar shearing strength was computed by taking the average values of those (the average of ○ and ● in the figure) whose inter-laminar shearing strength was constant regardless of the span among the data that underwent inter-laminar shearing failure. The difference between ○ and □ will be discussed later.

Figure 3 shows the apparent bending strength, σ_{max}, computed from equation (2) based on the failure load, P, when the span/thickness ratios (l/h) were varied. The bending strength was determined using the same method as for the inter-laminar shearing strength.

Table 2.
Comparison of inter-laminar shearing strength and bending strength between as-received and thermal shocked specimens

	τ (MPa)	Normalized τ(%)	σ (MPa)	Normalized σ(%)
As-received	12.4	100	232	100
Thermal shocked (3 times)	9.56	77.1	205	88.2

τ: interlaminar shearing strength; σ: bending strength.

Table 2 shows the result of comparing the inter-laminar shearing strength and the bending strength before and after the thermal shocks. Their normalized values with respect to those of the inter-laminar shearing strength and the bending strength before the thermal shocks are also shown in the table. It is seen that the inter-laminar shearing strength was reduced by more than 20% and the bending strength was reduced by more than 10% due to the thermal shocks.

The boundary between the inter-laminar shearing failure and the bending failure was examined next. In general, inter-laminar shearing failure occurs when the specimen span is short and bending failure occurs when the span is long. The theoretical boundary (l/h) between the inter-laminar shearing failure and the bending failure is given from equations (1) and (2) as
Boundary:

$$l/h = \frac{1}{2}\frac{\sigma_{\max}}{\tau_{\max}}. \tag{3}$$

This formula implies that the boundary is shifted toward the direction where l/h is larger when the reduction rate of the inter-laminar shearing strength, $\tau_{\max}$, is larger, and the boundary is shifted toward the direction where l/h is smaller when the reduction rate of bending strength, $\sigma_{\max}$, is larger. In this experiment, the reduction rate of inter-laminar shearing strength by the thermal shocks was larger, which implies the boundary shifted toward the direction with larger l/h values, and it is indeed seen that the values of l/h were shifted from around 10 to around 11 by the thermal shocks.

The theoretical boundary between the inter-laminar shearing strength and the bending failure was also computed. By substituting the experimental values in Table 2 into equation (3), we obtained $l/h = 9.35$ before the thermal shocks and $l/h = 10.7$ after the thermal shocks. As these values closely agree with those obtained by the sight and sound inspection, it can be concluded that the actual boundary between the inter-laminar shearing strength and bending failure lies in this neighborhood.

3.2. Influence of the number of thermal shocks

Figure 4 shows the relation between the inter-laminar shearing strength and the number of thermal shocks for $l/h = 8$ (○ and ● in Fig. 2) where the inter-laminar

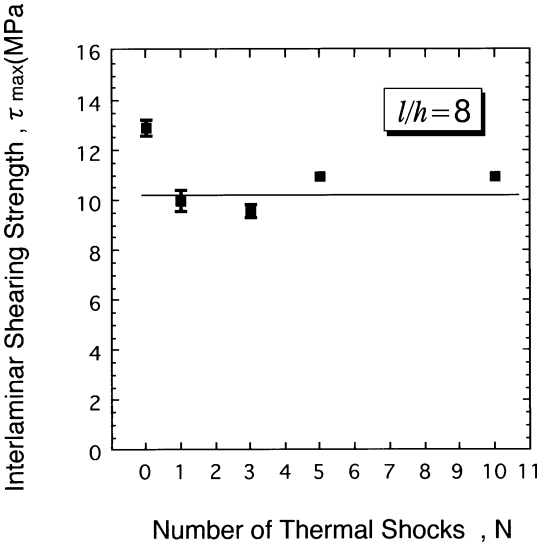

Figure 4. The influence of the number of thermal shocks on inter-laminar shearing strength.

shearing failure is stable. The experiment was conducted at a temperature lower than the final heat treatment temperature of the specimens (1500°C for the thermal shock temperature and 1600°C for the final heat treatment temperature) so that the matrix organization of the specimens would not change. From this result it is seen that the inter-laminar shearing strength was reduced significantly by the first thermal shock but no further strength degradation was observed. This tendency agrees with the report by Takahashi *et al.* [7] on the relation between the number of thermal shocks and the tensile strength.

3.3. Internal damage by thermal shocks

Figures 5–7 show the observation of internal damage due to the thermal shocks by scanning electron microscopy (SEM) and optical microscopy. Figure 8 shows a schematic view of the location of each picture and the damage morphology. It should be noted that it is necessary to distinguish the interfacial delamination between the 90° layer and the matrix (Fig. 6) from the inter-laminar delamination between the 0° layer and the 90° layer (Fig. 5). It is seen from Figs 5 and 6 that delamination took place at (A) the 0°/90° interface and (B) the 90°/matrix interface. Delamination at the (A) 0°/90° interface was observed for almost all interfaces but delamination at the (B) 90°/matrix interface was extremely rare.

Figure 7 shows a comparison of (C) transverse cracks. Although transverse cracks are already present in the specimens even before the thermal shocks, they are due to contraction during the manufacturing process or due to thermal stresses during the cooling process after manufacturing [8]. The number of transverse cracks did not increase due to the thermal shocks but opening of the transverse crack width

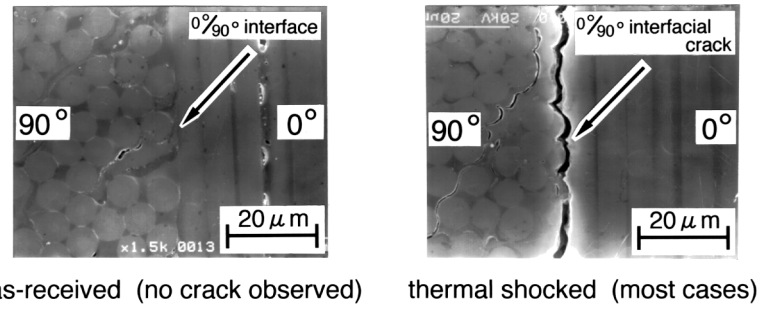

Figure 5. Comparison of 0°/90° interfacial crack.

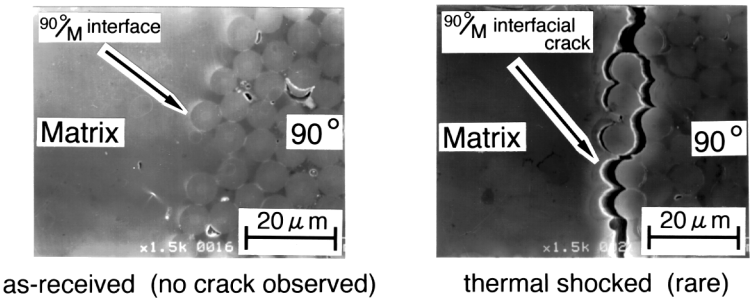

Figure 6. Comparison of 90°/matrix interfacial crack.

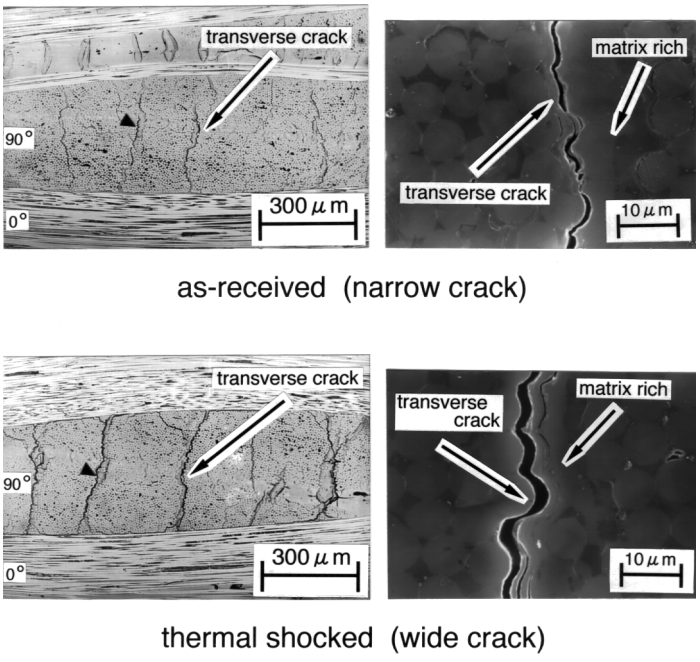

Figure 7. Comparison of transverse crack.

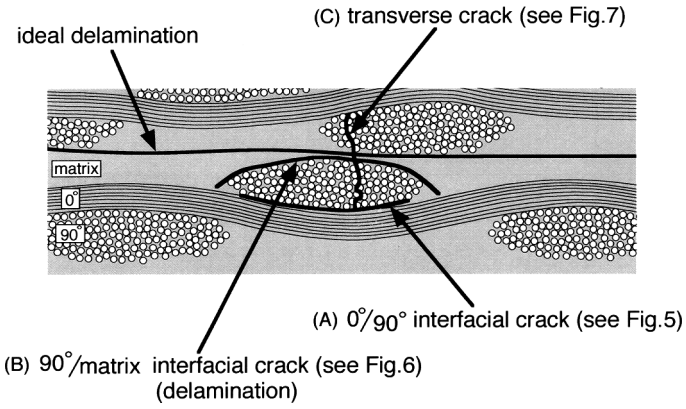

Figure 8. Schematic view of internal damage induced by thermal shocks.

Table 3.
Comparison of internal damage between as-received and thermal shocked specimens

	As-received	After thermal shock
0°/90° interfacial crack	no crack	most cases
90°/matrix interfacial crack	no crack	rare
transverse crack	narrow crack	wide crack

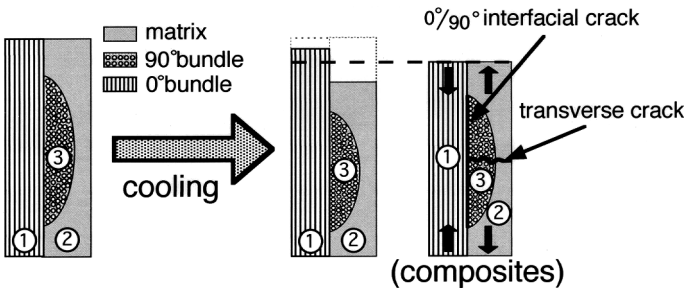

Figure 9. Schematic explanation for initiation of internal damage induced by thermal shocks.

was confirmed. It is also noted that the transverse cracks were present along the interface of the matrix-rich part within the 90° bundle.

Table 3 summarizes the damage induced by the thermal shocks. The mechanism of damage formation can be explained as follows (see Fig. 9): the thermal expansion coefficient of the matrix carbon ② of the test specimens was about $4 \times 10^{-6}\mathrm{K}^{-1}$ [9] which was almost the same as that in the radial direction (③ in the 90° direction) of the carbon fibers. On the other hand, the thermal expansion coefficient in the axial direction (① in the 0° direction) of the carbon fibers changed its sign from minus

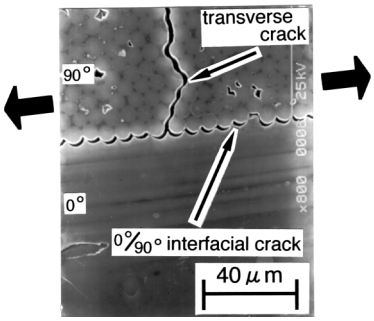

Figure 10. Release of residual thermal stress.

to plus at 400°C [10] and was still less than $2 \times 10^{-6}\mathrm{K}^{-1}$ even at 1500°C. For this reason, almost no thermal strain was generated at the 90°/matrix interface (③−②) during the temperature dropping process of the thermal shocks but larger thermal strain was generated at the 0°/90° interface (①−③) and the 0°/matrix interface (①−②). In addition, the thermal strain rate during the temperature dropping process of the thermal shocks was much larger than that during the cooling period in the manufacturing process. It can be concluded, therefore, that mismatch of the thermal expansion coefficients between the radial and axial directions of the carbon fibers caused the significant delamination at the 0°/90° interface (①−③), while almost no delamination was present at the 90°/matrix interface (③−②). However, if only the mismatch in the thermal expansion coefficients was to be considered, there should be significant delamination at the 0°/matrix interface (①−②). This is because it is a problem with the interfacial strength, and the strength at the 0°/matrix interface (①−②) of the test specimen was larger than the strength at the 0°/90° interface (①−③).

Figure 10 shows a magnified view of part of the 0°/90° interface (①−③) after the thermal shocks. It is seen from this figure that the delamination at the 0°/90° interface (①−③) actually released the thermal residual strain [11, 12] at the 0°/90° interface (①−③) generated during baking. It is therefore concluded that the opening of transverse cracks was caused by the release of thermal residual strains at baking at the 0°/90° interface.

3.4. Reduction of inter-laminar shearing strength by thermal shocks

Figure 11 shows photos of the test specimens after the inter-laminar shearing test ($l/h = 8$) and Fig. 12 shows a schematic view of the damage. By comparison of the failure morphology before and after the thermal shocks, it was confirmed that damage in the matrix near the loading nose and at the 90° layer was very significant before the thermal shocks, and some of cracks induced by such damage became the initiation point of the inter-laminar shearing failure. It has been reported [13] that inter-laminar shearing failure in woven C/C composites started propagating

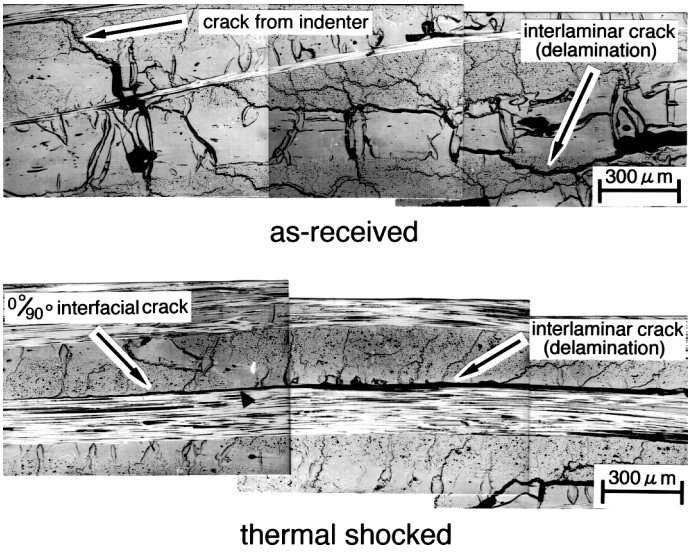

Figure 11. Comparison of inter-laminar shearing failure.

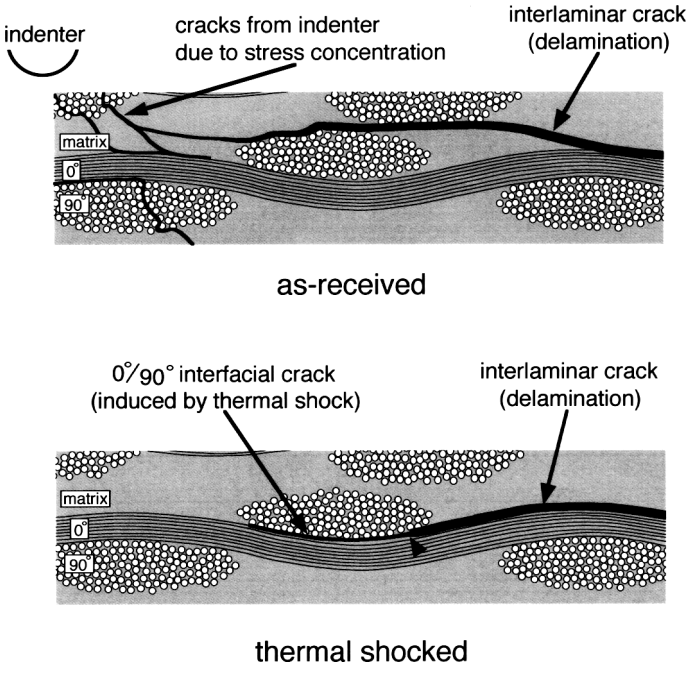

Figure 12. Schematic view of inter-laminar shearing failure.

around the neutral axis of the center part between the loading nose and the support point, but actual failure is believed to begin generally around the loading nose in the three-point bending test, because a high shear stress concentration took place

near the loading nose [14]. As was mentioned before, the test specimens in this experiment were fabricated by the resin soaking method and voids in the matrix were densified by coal-tar pitch, which implies that the part near the loading nose may be the initiation point of failure.

On the other hand, it was confirmed that inter-laminar shearing failure occurred by the delamination at the 0°/90° interface after the thermal shocks. Taking into account that the delamination at the 0°/90° interface lay in the same direction as the inter-laminar shearing stress, it can be concluded that the reduction of the inter-laminar shearing strength induced by the thermal shocks was caused by the delamination at the 0°/90° interface acting as the initiation point of inter-laminar shearing failure.

3.5. Reduction of bending strength due to thermal shocks

Figure 13 shows a comparison of load–displacement curves before and after the thermal shocks. Reduction of bending strength due to the thermal shocks is clearly seen. If damage such as failure in fibers is confirmed by thermal shocks, it may be a degradation factor of the ideal bending rigidity (reduction of bending strength). However, most of what was observed were delaminations at the 0°/90° interface and there was no significant difference in morphology of bending failure before and after the thermal shocks induced by the delamination. As transverse cracks hardly affect the bending strength [15], it can be concluded that the cause of reduction of bending rigidity (reduction of bending strength) was not because of internal damage such as microcracks induced by thermal shocks as the initiation point of failure. For this reason, a beam structure called a 'piled up beam' was considered. The principle of the piled up beam is to stack simple beams, and its bending rigidity is known to be much lower than that of an integrated composite beam. A significant amount

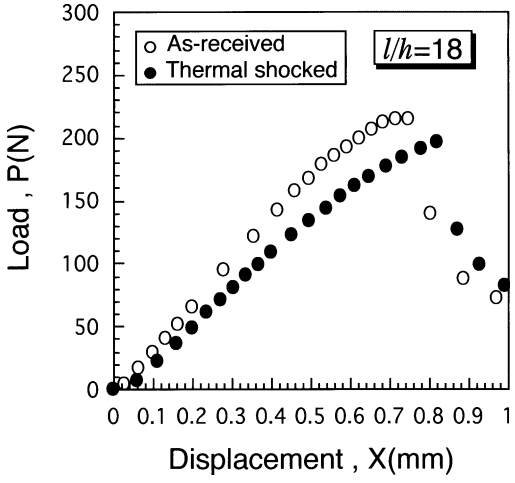

Figure 13. Comparison of load–displacement curve.

of delamination at the 0°/90° interface was observed in this experiment, and it is believed that the beam with such delamination after the thermal shocks had the elements of piled up beams at these places. This way, it follows that the bending strength after the thermal shocks was reduced because the bending rigidity of a beam after a thermal shock was significantly reduced.

3.6. Inter-laminar shearing failure behavior due to difference of l/h

As was mentioned above, the theoretical inter-laminar shearing strength at inter-laminar shearing failure is constant independent of the span but a difference in the inter-laminar shearing strength was observed in this experiment which depended on l/h (see Fig. 2). The inter-laminar shearing strength was constant for $l/h = 7-10$ but exhibited very large values when l/h was relatively small, in the range $l/h = 4-6$. The inter-laminar shearing strength for a unidirectional CFRP was also constant for $l/h = 5-8$ and showed very large values for $l/h = 4$ under a similar test. It is believed in general that the smaller the value of l/h, the larger the inter-laminar shearing strength independent of the material or composition [4] and this experiment also agreed with this.

An internal observation after the experiment by optical microscopy was also conducted for $l/h = 5$. It was confirmed that damage was severe around the loading nose and near the support point (in particular near the loading nose) and cracks were seen extending over multiple layers. Most of the cracks were cut off in the middle. This failure morphology was quite different from the 'inter-laminar shearing failure (simple shearing failure) in which inter-laminar cracks were generated around the neutral axis'. One of the possible reasons for this is that there was compression in the thickness direction in the test specimen if a span was extremely short such as $l/h = 0$ but propagation of the inter-laminar shearing cracks was also prevented even for $l/h = 5$ as the influence by the compression was large. For this reason, a significantly larger inter-laminar shearing strength was observed at $l/h = 4-6$ compared with $l/h = 7-10$.

The inter-laminar shearing strength of the plain woven C/C composite in this experiment was obtained using $l/h = 8$ for the reason mentioned above. However, this value of l/h is not to be recommended for all C/C composites in other strength tests. If, however, the value of l/h is too small, the inter-laminar shearing strength tends to be overestimated. Thus, when inter-laminar shearing failure takes place even for a large value of l/h ($l/h > 5$), it is recommended that values of l/h near that value should be used for the inter-laminar shearing strength in order to avoid the influence of l/h.

4. CONCLUSIONS

The inter-laminar shearing strength and bending strength before and after thermal shocks were compared and examined as factors influencing the effects of thermal shocks on woven C/C composites. The following conclusions are drawn:

(1) The thermal shock brought significant delaminations at the interface of the axial and radial directions ($0°/90°$ interface) with different thermal expansion coefficients. It was confirmed that the thermal residual strain generated at baking in the manufacturing process was released by this delamination.

(2) Both the bending strength and the inter-laminar shearing strength were reduced by the thermal shocks but the reduction in the inter-laminar shearing strength was larger. This is because the reduction in the inter-laminar shearing strength was due to the delamination at the $0°/90°$ interface becoming an initiation point of the inter-laminar shearing failure, and the reduction in the bending strength was due to the reduction of bending rigidity because of the delamination at the $0°/90°$ interface. The inter-laminar shearing strength became constant once a thermal shock was applied regardless of the number of shocks.

(3) The inter-laminar shearing strength at the inter-laminar shearing failure varied for different l/h values. Inter-laminar shearing tests are, in general, conducted at around $l/h = 5$ by adopting the CFRP standard (JIS K 7078, the interlaminar shearing test method of carbon fiber reinforced plastic) but in this experiment, very complex failure morphology was present at around $l/h = 5$ and it is believed that the values of $l/h = 7–10$ should be more appropriate for testing purposes.

REFERENCES

1. J. Takahashi, J. Watanabe, H. Tsuda, K. Kemmochi, R. Hayashi and H. Fukuda, Ultra high temperature properties of advanced Carbon/Carbon composites (Development of testing equipment and the influence of thermal shock on the properties), *J. Natl. Institute of Mater. and Chem. Research (NIMC)* **4** (6), 213–222 (1996) (in Japanese).
2. *Proc. Symposia on High Performance Materials for Severe Environments*, 1st (1990)–8th (1997) (in Japanese).
3. Y. Ishiguro, T. Akatsu, H. Ishii, Y. Tanabe and E. Yasuda, Evaluation of the shear strength of a C/C composite using various testing methods, in: *Proc. 1996 Annual Meeting of JSCM*, pp. 71–72 (1996) (in Japanese).
4. Japanese Industrial Standard, *JIS K 7078*, Commentary, p. 6 (1991) (in Japanese).
5. J. Takahshi, K. Kemmochi, J. Watanabe, H. Fukuda and R. Hayashi, Development of ultra-high testing equipment and some mechanical and thermal properties of advanced carbon/carbon composites, *Adv. Composite Mater.* **5** (1), 73–86 (1995).
6. H. Hatta, Y. Kogo and T. Yarii, Oxidation resistance of C/C composites, in: *Proc. 1995 Annual Meeting of JSCM*, pp. 67–68 (1995) (in Japanese).
7. J. Takahashi, J. Watanabe, H. Tsuda, K. Kemmochi, R. Hayashi and H. Fukuda, Ultra-high temperature properties for C/C composites, in: *Progress in Advanced Materials and Mechanics*, W. Tzuchiang and T. W. Chou (Eds), pp. 1032–1037. Peking University Press (1996).
8. Y. Kogo, H. Hatta, A. Okura, M. Fujikura and Y. Seimiya, Flexural and Interlaminar Shear Properties of C/C Composite at Elevated Temperatures, *TANSO* (166), 41 (1995) (in Japanese).
9. S. Otani, K. Okuda and S. Matsuda, in: *Carbon Fibers*, p. 82. Kindai Henshu-sha, Tokyo (1984) (in Japanese).
10. A. Kohyama, H. Serizawa and S. Sato, Recent trends of research on C/C composites, *J. Japan Soc. Compos. Mater.* **22**, 91–99 (1996) (in Japanese).

11. J. Takahashi, H. Tsuda, K. Kemmochi, O. Okuda and T. Ogasa, Microscopic studies on the strength of C/C composites, in: *Proc. 8th Symposium on High Performance Materials for Severe Environments*, pp. 427–435 (1997) (in Japanese).
12. G. Chollon, J. Takahashi and K. Kemmochi, Raman microspectroscopy study of a C/C composite, in: *Proc. 5th Japan Intern. SAMPE Symp.*, pp. 1567–1572 (1997).
13. P. D. Copp, J. C. Dendis and S. Mall, Failure analysis and damage initiation in carbon-carbon composite materials under three-point bending, *J. Compos. Mater.* **25**, 593–608 (1991).
14. M. Uemura, Some aspects of mechanical property test methods for FRP and design criteria, *J. Japan Soc. Compos. Mater.* **7**, 32–39 (1981) (in Japanese).
15. Y. Kogo, H. Hatta, A. Okura, M. Fujikura and Y. Seimiya, Flexural and Interlaminar Shear Properties of C/C Composite at Elevated Temperatures, *TANSO* (166), 40–46 (1995) (in Japanese).